The Franck-Condon approximation for second-order Jahn-Teller vibronic reduction in icosahedral T⊗h systems

2002 J. Phys.: Condens. Matter 14 3115

(http://iopscience.iop.org/0953-8984/14/12/304)

INSTITUTE OF PHYSICS PUBLISHING JOURNAL OF PHYSICS: CONDENSED MATTER

J. Phys.: Condens. Matter **14** (2002) 3115–3127 PII: S0953-8984(02)32953-9

The Franck–Condon approximation for second-order Jahn–Teller vibronic reduction in icosahedral T ⊗ h systems

Michel Abou-Ghantous[1], Victor Z Polinger[2], Janette L Dunn[2] and Colin A Bates[2]

[1] Physics Department, American University of Beirut, Beirut, Lebanon
[2] School of Physics and Astronomy, University of Nottingham, University Park, Nottingham NG7 2RD, UK

E-mail: Janette.Dunn@nottingham.ac.uk and Colin.Bates@nottingham.ac.uk

Received 23 January 2002
Published 15 March 2002
Online at stacks.iop.org/JPhysCM/14/3115

Abstract

The Franck–Condon (FC) approximation is used to obtain analytical values for the second-order factors describing vibronic reduction for the case of the strongly coupled icosahedral $T_{1u} \otimes h_g$ Jahn–Teller (JT) system in which an electronic triplet ground state is coupled to vibrations of fivefold degeneracy. This is believed to be applicable to the ground state of the C_{60}^{-} ion and so the calculations should help in providing valuable physical information on this fullerene ion. The procedures for determining vibronic reduction effects depend critically on the particular JT system and upon the vibronic coupling strength. In the FC approximation, the major contributions to these reduction factors originate from virtual vertical transitions between the ground electronic adiabatic state and excited vibronic states associated with upper sheets in the adiabatic potential energy surface. At strong coupling, other transitions may be neglected. The FC results are compared with those obtained from an alternative approach involving a shift transformation. Details are given for perturbations containing orbital operators of threefold (T_1) and fivefold (H) symmetry. The discussion emphasizes the inherent high symmetry of the system.

1. Introduction

The energy spectrum and electronic properties of degenerate electronic states are often much influenced by the coupling to vibrations of their surroundings. This is seen particularly in spectroscopic and bulk measurements of systems involving C_{60}, in which coupling of the electrons to the vibrating molecular cage takes place [1]. This vibronic coupling manifests itself through the Jahn–Teller (JT) effect [2]. This can modify the size and character of

any electronic perturbations that may be present. Examples of perturbations which can be introduced in this way include spin–orbit coupling, random strains, and external stress. In order to interpret data from spectroscopic experiments, for example, the energy levels responsible for the observed lines must be determined. It is convenient therefore to introduce the concept of the effective Hamiltonian [3–6]. This contains additional parameters that multiply the orbital operators contained within the perturbation into which the vibronic coupling has been transferred. These parameters are called vibronic reduction factors (RFs) [7–12]. They arise from the involvement of the phonons which makes the effective mass of the electrons larger. This in turn reduces the energy gaps in the energy spectrum of the electrons. If the perturbation is sufficiently weak compared to the vibronic coupling that it can be considered in first order, the corresponding factor is called a first-order RF. Similarly, second-order terms involving the perturbation in second order (either the same perturbation twice or as a product of two different perturbations) introduce the corresponding second-order RFs. Second-order RFs are important as they can generate contributions significantly larger than and different from those in first order [13, 14].

First-order RFs are relatively simple to calculate [7] but second-order RFs involve coupling to an infinite set of excited vibronic states. They can only be calculated exactly in the pure adiabatic case in which there is no mixing of the electronic states, such as that in the case of the cubic $T \otimes e$ JT system in which an orbital triplet (T) interacts with the doubly degenerate e-type vibrations [15]. In all other cases, approximations have to be introduced. Details of the underlying theory and calculations from it can be found in [16–19], for example.

In most approaches to interpreting experimental data, RFs are treated as adjustable parameters with values chosen to fit the data. However, these RFs contain a lot of important physics. Indeed, the absence of a general theory of vibronic effects in fullerenes covering the full range of coupling strengths slows down advance in this important area. We recall that in earlier work on magnetic ion impurities in insulating and semiconducting host crystals, it was only by combining theoretical work involving the influence of the JT effect on various perturbations that many of the unknown impurities could subsequently be unambiguously identified. It was shown that the effects of random strain combined with both first- and second-order RFs were fundamental to this understanding and identification. These development were spread over many years and involved much interplay between theoreticians and experimentalists. Fullerene research is relatively young and thus we are attempting to build up some fundamental principles which will assist in bridging the gap between basic theory and experimental work. The latter include fluorescence emission spectroscopy, Raman spectroscopy, electron paramagnetic resonance (EPR) and the observed magnetic and superconducting properties of the fullerides. Specific recent examples include an analysis of magnetic ordering in TDAE-C_{60} [20], the A_3C_{60} fullerides [21], and the observation via EPR of C_{60} molecules embedded in a crystal field [22]. A recent general review [23] discusses how the vibronic and spin–vibronic angular momenta couplings combined with the JT effect influence the dynamic properties of molecular systems.

The ground state of the C_{60}^{-} ion is an electronic T_{1u} triplet, which couples to the icosahedral fivefold-degenerate h_g modes of vibration of the fullerene cage. It will therefore be subject to a $T_{1u} \otimes h_g$ JT effect. A calculation of the first- and second-order RFs for the $T_{1u} \otimes h_g$ JT system has recently been given using a shift transformation (ST) approach [24]. Results apply to spin–orbit coupling and other perturbations. In this method, the states are assumed to be a linear combination of shifted oscillator states. Whilst this is a good approximation for the ground states, it may not be appropriate for the higher-lying excited states. As second-order RFs involve coupling to an infinite manifold of excited states, this means that the RFs calculated using this method may be inaccurate. As we move to excited states with higher energy, the

energy denominators of the RFs increase. At the same time, the overlaps between the states in different wells decrease. This indicates that the excited states should become increasingly less important as their energy increases. Nevertheless, we need to determine whether all of the excited shifted oscillator states in each well should be used in the summation. Numerical approaches to second-order RF calculations fail to provide reasonable results because they are even less applicable to highly excited states than the ST results.

The aim of the present paper is to use the Franck–Condon (FC) approximation [25, 26] to calculate the effects of vibronic reduction in the $T_{1u} \otimes h_g$ JT system. In this approximation, it is assumed that virtual transitions between the ground and excited states, as occur within the second-order perturbation formulae, take place so rapidly that the nuclei do not change their positions during a transition. This will be true if the energy gaps in the nuclear system are much larger than the energy gaps within the electronic system [27]. This is the case in the region of strong coupling, and therefore the FC approximation will be valid in this limit. In general, when the FC approximation is used to solve problems, the Born–Oppenheimer approximation [2] is employed and applied to second-order perturbation terms involving factored adiabatic wavefunctions. A recent text [28] has given some relevant general details of the FC approximation, whilst a very recent paper [29] encompasses the FC approximation in an analysis of the angle-resolved photoemission spectra predicted for $LaMnO_3$. However, the detailed procedures on how to use this approximation depend critically on the particular application.

The next section (2) outlines the general theory of vibronic reduction with comments on how it can be applied to the $T_{1u} \otimes h_g$ JT system. It introduces the effective Hamiltonian and defines the basic quantities needed. Section 3 describes how the FC approximation may be used to evaluate the second-order RFs. The results are given and compared with the previous results obtained using the ST method in section 4. Further considerations involving the ST results are given in section 5. A full discussion of the results follows in section 6.

2. The effective Hamiltonian

In order to proceed, we need some basic expressions from the general theory of vibronic RFs; the detailed derivation of these expressions and thorough discussions of their physical meanings can be found in [1, 2, 24], for example.

2.1. The basic vibronic Hamiltonian

The Hamiltonian $\mathcal{H}$ of a general vibronic system consists of the sum of the kinetic and elastic energies together with potential energy associated with the coupling of the electronic motion with the nuclear vibrations. The coupling comprises a linear term $V_l \sum_\gamma Q_{\Gamma\gamma} C_{\Gamma\gamma}$ and any contributions from quadratic coupling. The parameter V_l is the linear coupling constant, $C_{\Gamma\gamma}$ is the electronic operator transforming as $\Gamma\gamma$, and $Q_{\Gamma\gamma}$ is the corresponding vibrational coordinate of the nuclear frame (or molecule in the case of C_{60}) having reduced mass μ and frequency ω. In the $T_{1u} \otimes h_g$ JT system, the electronic label $\Sigma \equiv T_{1u}$ with components $\sigma_j = \{x, y, z\}$ and the oscillators $\Gamma \equiv h_g$ with the sum γ taken over the five components of the h_g vibrational mode. The orbital states are written in the form $|\Sigma\sigma_j)$. The $C_{\Gamma\gamma}$ are thus given in general by

$$C_{\Gamma\gamma} = \sum_{\sigma_i \sigma_j} |\Sigma\sigma_j)(\Sigma\sigma_i|\langle\Gamma\gamma\,\Sigma\sigma_i|\Sigma\sigma_j\rangle. \tag{1}$$

The Clebsch–Gordan coefficients $\langle\Gamma\gamma\,\Sigma\sigma_i|\Sigma\sigma_j\rangle$ are tabulated in [30]; explicit expressions for them in terms of 3×3 matrices with respect to the orbital basis $\{x, y, z\}$ for $\Sigma = T_{1u}$ are given in [24].

With just linear coupling, the lowest adiabatic potential energy surface (APES) of the $T_{1u} \otimes h_g$ system, to be referred to as the ground sheet, forms a trough of energy $-E_{JT}$, where E_{JT} ($=V_1^2/5\mu\omega^2$) is the JT stabilization energy [24]. (The zero of energy is defined by taking $V_1 = 0$.) However, when quadratic coupling is introduced, this trough is warped such that wells are formed [31–33]. The wells will be labelled by the index k. There are either ten wells of symmetry D_{3d} or six wells of symmetry D_{5d}, depending upon the relative magnitudes of the two quadratic coupling constants [34].

The ground states of the system are those in which the nuclear motion is localized about the lowest-energy wells. We assume that any anharmonicity in the wells, which increases with energy, can be neglected for the ground state. The nuclear functions in the wells in the ground sheet then show oscillatory behaviour. As wells of a given symmetry are equivalent to each other, tunnelling between equivalent wells can take place. The ground states are therefore a linear combination of well states. Appropriate combinations can be found from symmetry considerations [24, 34, 35]. The degeneracy of the well states is partially lifted and a T_1 triplet ground state is restored. The remaining states form tunnelling levels with energies just above that of the ground state. In the ST method, the ground state in well k is denoted by $|\psi_k'; 0\rangle$, and the symmetry-adapted ground states that take account of tunnelling between wells are called $|0, T_1\sigma_j\rangle$ where $j = \{x, y, z\}$. Consequently,

$$|0, T_1\sigma_j\rangle = \sum_k c_k^j |\psi_k'; 0\rangle \tag{2}$$

where the '0' indicates that the localized oscillators are in their ground states. The c_k^j are coefficients subject to the normalization condition

$$\sum_k |c_k^j|^2 = 1. \tag{3}$$

The energy of the symmetry-adapted ground state will be called E_0^0.

We now need some notation to refer to all of the excited states. This includes states with $n \geqslant 1$ phonon excitations associated with the ground sheet and states with $n \geqslant 0$ phonon excitations on the two excited sheets. These will be referred to using the notation $|i, n\rangle$ where $i = 0$ corresponds to the ground sheet and $i = 1, 2$ to the excited sheets. This notation ignores any degeneracies but, as we show later, details of these states do not enter the calculations, so this is not important. The energy of the state $|i, n\rangle$ will be denoted by E_i^n [2].

In the adiabatic approximation, the states $|i, n\rangle$ can be written in the form

$$|i, n\rangle = |\Psi_i(r, Q))|\Phi_n^i(Q)\} \tag{4}$$

where $|\Psi_i(r, Q))$ is the electronic wavefunction written as a function of the position r and vibrational parameter Q, and $|\Phi_n^i(Q)\}$ is the nuclear wavefunction.

2.2. Vibronic reduction factors

Before giving detailed expressions for second-order vibronic RFs, we will illustrate the need for such factors in physical terms. In a system in which the electrons are strongly coupled to their surroundings, the electrons behave as if they are coated with phonons. They are thus much heavier, so transitions from one ground state to another ground state caused by a perturbation become weaker as the coupling gets stronger. This first-order reduction is often sufficiently strong that it may virtually cancel any transition in first order. Virtual transitions via the excited states then become more probable and thus there is a need to calculate the magnitude of these reductions in both first and second order, and to compare the two.

If the Hamiltonian of an (electronic) perturbation having symmetry Γ_a within the ground state is written as

$$\mathcal{H}^{(1)}(\Gamma_a) = \sum_{\gamma} W_{\Gamma\gamma} C_{\Gamma\gamma} \tag{5}$$

where $W_{\Gamma\gamma}$ are coefficients, then second-order perturbation theory generates a Hamiltonian of the form [16]

$$\mathcal{H}^{(2)}(\Gamma_a \otimes \Gamma_b) = \mathcal{H}^{(1)}(\Gamma_a) G(T_1) \mathcal{H}^{(1)}(\Gamma_b) \tag{6}$$

where $G(T_1)$ is the Green operator

$$G(T_1) = \sum_{i,n} \frac{|i,n\rangle\langle i,n|}{E_0^0 - E_i^n} \tag{7}$$

involving the excited states $|i, n\rangle$ (which exclude $i = n = 0$).

The next stage is to express the effect of the perturbation given in equation (5) by appropriate first- and second-order effective Hamiltonians. The detailed derivation of these expressions and a thorough discussion of their physical meaning can be found in [24], for example. To summarize the procedures, we may represent the effect of perturbations using effective Hamiltonians of the form

$$\mathcal{H}^{(1)}_{eff} = K^{(1)}_{M}(\Gamma_a) \sum_{\gamma} W_{\Gamma\gamma} C_{\Gamma\gamma}$$

$$\mathcal{H}^{(2)}_{eff}(\Gamma_a \otimes \Gamma_b) = \sum_{\gamma_a\gamma_b} \sum_{Mm} W^{+}_{\Gamma\gamma_a} W_{\Gamma\gamma_b} \langle \Gamma\gamma_a\Gamma\gamma_b|Mm\rangle K^{(2)}_{M}(\Gamma_a \otimes \Gamma_b) L^{(2)}_{Mm}(\Gamma_a \otimes \Gamma_b) \tag{8}$$

where M is contained in the product $\Gamma_a \otimes \Gamma_b$,

$$K^{(2)}_{M}(\Gamma_a \otimes \Gamma_b) = \frac{\langle 0, T_1\sigma_i|\mathcal{L}^{(2)}_{Mm}(\Gamma_a \otimes \Gamma_b)|0, T_1\sigma_j\rangle}{(T_1\sigma_i|L^{(2)}_{Mm}(\Gamma_a \otimes \Gamma_b)|T_1\sigma_j)} \tag{9}$$

and

$$\mathcal{L}^{(2)}_{Mm}(\Gamma_a \otimes \Gamma_b) = \sum_{\gamma_i\gamma_j} C_{\Gamma\gamma_i} G(T_1) C_{\Gamma\gamma_i} \langle \Gamma\gamma_i\Gamma\gamma_j|Mm\rangle. \tag{10}$$

$L^{(2)}_{Mm}$ is obtained directly from $\mathcal{L}^{(2)}_{Mm}$ by replacing $G(T_1)$ with unity. The components σ_i and σ_j are chosen appropriately, so that the numerator and denominator in equation (9) are non-zero.

The effective Hamiltonians in equations (8) contain only electronic operators, whereas the real Hamiltonians given in equations (5) and (6) also include vibrational terms. The vibrational nature of the ground states has been 'transferred' to the set of so-called first-order RFs $K^{(1)}_{M}(\Gamma_a)$ and second-order RFs $K^{(2)}_{M}(\Gamma_a \otimes \Gamma_b)$.

3. Evaluation of the vibronic reduction factors within the FC approximation

We will now introduce the FC approximation. We start by replacing the vibronic well state $|\psi'_k; 0\rangle$ in equation (2) by a product of electronic and nuclear wavefunctions $|\psi_k(r, Q))|\phi_k(Q)\}$, just as was done for the excited states in equation (4). $|\psi_k(r, Q))$ is the orbital ground state in well k and $|\phi_k(Q)\}$ is the associated five-dimensional oscillator function centred about $Q = Q^k_0$. The latter is given by

$$|\phi_k(Q)\} = (\pi/\tau)^{5/2} \exp[-\tau(Q - Q^k_0)^2] \tag{11}$$

where $\tau = m\omega/(2\hbar)$ and where ω is the frequency of the corresponding normal mode including the effects of anisotropy in the wells. This is the so-called crude adiabatic [36] or Born–Oppenheimer [2] approximation. This terminology is used as the adiabatic electronic

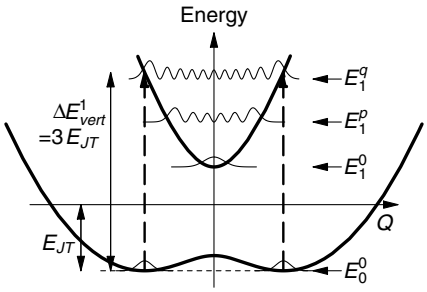

Figure 1. A one-dimensional FC diagram showing the cross-section in the plane joining two D_{5d} wells in the lowest sheet of the $T_{1u} \otimes h_g$ problem. The thick solid curves show the lowest sheet containing the two wells and one of the two excited sheets (labelled '1'). The ground states in the wells on the lowest sheet are shown together with the ground state and two of the infinite number of possible excited states, labelled p and q, on the upper sheet. The vertical FC transitions from one of the ground states are indicated by dashed arrows. Only states near q have significant overlap with the ground state. The energies indicated are defined in the text.

wavefunctions $|\psi_k(r, Q))$ depend smoothly on Q. In contrast, the ground-state oscillator functions $|\phi_k(Q)\}$ are relatively very sharp. This enables us to replace $|\psi_k(r, Q))$ with $|\psi_k(r, Q_0^k))$. The physical reason for this is that the nuclear masses are so large that the delta-function-like wavefunction for the nuclei effectively constrains the nuclear motion to the bottom of the wells to give static-type behaviour. The larger the vibronic coupling, the more accurate the Born–Oppenheimer approximation becomes. The mathematical criterion for this approximation to apply is that $\hbar\omega \ll E_{JT}$. The right-hand side of this inequality is proportional to V_1^2. This approximation provides a basis for calculating values for the RFs in the strong-coupling case when a large number of excited states need to be considered.

The basic idea of the FC approximation can be understood in terms of WKB wavefunctions. The excited vibronic states with high excitation energy oscillate as $\exp(\mathrm{i}PQ)$, where $P = \sqrt{2m(E-U)}$ is the linear momentum of the 'particle', E is its total energy, and $U(Q)$ is the corresponding potential energy. Due to these oscillations, the dominant contribution to the overlap integral with a smooth function originates from turning points, where $P = 0$. As mentioned above, the other factor in the integrand is the δ-function-like ground-state wavefunction. Evidently, the product is zero unless the two (almost) singular points, the turning point in the excited state and the equilibrium position of the ground state, coincide. Therefore, all transitions to excited vibronic states can be ignored except for the vertical transitions to the upper sheets; all other transitions have negligibly small overlap integrals. This situation is illustrated schematically in figure 1, which plots the ground sheet and one of the excited sheets in the plane containing two of the D_{5d} minima. The vertical transitions are indicated by dashed arrows. It should be noted that the WKB approximation is not a necessary component of the FC approximation, and its criteria do not actually apply to the FC approximation. It has been used above just to illustrate the main ideas behind the FC approach. Due to the arguments given above, the energy denominator in equation (7), which in general is different for each excited state $|i, n\rangle$, can then be replaced by the vertical energy gap ΔE^i_{vert} separating the sheets at $Q = Q_0^k$. This is a constant for each sheet i. For the $T_{1u} \otimes h_g$ problem, the gaps equal $3E_{JT}$. This leaves the contribution to the numerator of the Green operator due to sheet i of

$$\sum_n |\Phi_n^i(Q)\}\{\Phi_n^i(Q')| = \delta(Q - Q'). \tag{12}$$

The sum over the excited vibronic states has therefore been convoluted into the delta function $\delta(Q - Q')$. Therefore, $G(\mathrm{T}_1)$ in equation (10) can be replaced by the FC Green operator $G_{FC} \equiv G_{FC}(r, r', Q, Q_0^k)$ given by

$$G_{FC} = -\sum_i \frac{|\Psi_i(r, Q))(\Psi_i(r', Q')|}{\Delta E^i_{vert}} \delta^i(Q - Q') \tag{13}$$

where the 'i' on the δ-function indicates the sheet to which it applies. The sum is over the adiabatic electronic states on the two excited sheets $i = 1, 2$ rather than being a sum over an infinite number of vibronic excited states.

We note that the ground state involved in the determination of the RFs encompasses the ground states for each well as given by equation (2). However, the major contributions to the second-order RFs come from terms that are diagonal with respect to that well. In other words, a vertical transition that starts from a certain well will end up within the same well. The off-diagonal contributions are exponentially small as they are proportional to the corresponding overlap integral, which, at strong coupling, can be neglected. This result gives the physical background to the FC approximation; as the nuclei are much heavier than electrons, the virtual electron transition takes place in a time much shorter than the characteristic time of the nuclear motion. Therefore, to a good approximation, the latter do not move at all and hence transitions up to excited states and back down to the ground state are vertical.

As inter-well transitions can be neglected, the calculation of RFs reduces to the consideration of each well separately. We can write down a FC Green operator $G^{(k)}_{FC}$ for each well k, using these operators appropriately when calculating the matrix elements between a ground state in a well and an excited state needed to evaluate equation (9). As the electronic states in any well form a complete set, the closure relation can be used to obtain the result

$$G^{(k)}_{FC} = -[1_k - |\psi_k(r, Q_0^k))(\psi_k(r', Q_0^k)|]/\Delta E^i_{vert} \tag{14}$$

where 1_k stands for unity associated with well k. This expression now depends only on the adiabatic electronic state in well k.

4. The results

As ΔE^i_{vert} is directly proportional to V_1^2, the product $V_1^2 K_{\mathrm{M}}^{(2)}(\Gamma_{\mathrm{a}} \otimes \Gamma_{\mathrm{b}})$ is independent of V_1 and is a more appropriate quantity to use than $K_{\mathrm{M}}^{(2)}(\Gamma_{\mathrm{a}} \otimes \Gamma_{\mathrm{b}})$ by itself. Ham [7, 15] discussed a similar asymptotic behaviour of second-order RFs for the exact cubic T ⊗ e system that was considered originally; this same result was also obtained from the modelling of other linear systems having cubic symmetry (e.g. [16]). If the second-order coupling terms are included in the original Hamiltonian, ΔE^i_{vert} depends upon V_1^2 in a more complex way, and $V_1^2 K_{\mathrm{M}}^{(2)}(\Gamma_{\mathrm{a}} \otimes \Gamma_{\mathrm{b}})$ is no longer independent of V_1^2. However, $V_1^2 K_{\mathrm{M}}^{(2)}(\Gamma_{\mathrm{a}} \otimes \Gamma_{\mathrm{b}})$ still provides a useful way of quantifying the vibronic reduction effects. We restrict our discussion here to the linear coupling terms only.

Values for $V_1^2 K_{\mathrm{M}}^{(2)}(\Gamma_{\mathrm{a}} \otimes \Gamma_{\mathrm{b}})$ have been evaluated firstly for the cases in which $\Gamma_{\mathrm{a}} \equiv \Gamma_{\mathrm{b}} \equiv \mathrm{T}_1$ (e.g. representing spin–orbit coupling, for example), and secondly for $\Gamma_{\mathrm{a}} \equiv \Gamma_{\mathrm{b}} \equiv \mathrm{H}$.

4.1. The case of $\Gamma_a \equiv \Gamma_b \equiv T_1$

As the direct product $\mathrm{T}_1 \otimes \mathrm{T}_1 = \mathrm{A} \oplus \mathrm{T}_1 \oplus \mathrm{H}$, the symmetry component M can take the labels A, T_1 and H in this case. The calculation in this case is straightforward, as the T_1 orbital operator has zero diagonal matrix elements within the electronic ground state $|\psi_k)$ of all $\mathrm{D}_{3\mathrm{d}}$

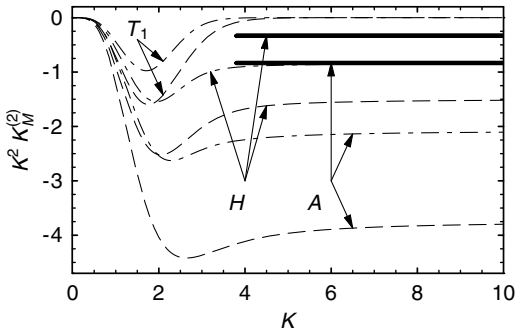

Figure 2. A plot of the calculated second-order RFs (in the form $K^2 K_{\mathrm{M}}^{(2)}$) as a function of K for perturbations of T_1 symmetry. The solid lines give results from the FC approximation; the dashed and dot–dashed curves are the results obtained from the ST method using $\mathrm{D}_{3\mathrm{d}}$ wells and $\mathrm{D}_{5\mathrm{d}}$ wells respectively. The labels give the values of M.

and $\mathrm{D}_{5\mathrm{d}}$ wells, so the second term in equation (14) is zero. On substituting the first term of the same equation into equations (8), we find that in general (i.e. for an operator of symmetry M),

$$K_{\mathrm{M}}^{(2)}(\mathrm{T}_1 \otimes \mathrm{T}_1) = -K_{\mathrm{M}}^{(1)}(\mathrm{T}_1)/\Delta E_{vert}^{i}. \tag{15}$$

A similar relation between first- and second-order RFs was found previously (see [17], equation (4.7)) in the case of cubic systems. As $K_{\mathrm{M}}^{(1)}(\mathrm{T}_1) = 0$, the only non-zero second-order RFs are those for which M = A and H.

To facilitate direct comparison with other published data, we introduce the dimensionless linear vibronic coupling parameter K (defined as k_1 in [24]) given by

$$K = -V_1/(2\hbar\mu\omega^3)^{1/2} = [5E_{JT}/(2\hbar\omega)]^{1/2} \tag{16}$$

and calculate instead $K^2 K_{\mathrm{M}}^{(2)}(\mathrm{T}_1 \otimes \mathrm{T}_1)$ as a function of K. As expected from the analysis above, the results from the FC approximation are horizontal straight lines in the figures. Also, results obtained from the $\mathrm{D}_{5\mathrm{d}}$ wells are exactly the same as those obtained from $\mathrm{D}_{3\mathrm{d}}$ wells. Figure 2 gives the results obtained for the case in which the ground-state minima are assumed to be of $\mathrm{D}_{3\mathrm{d}}$ symmetry. It also shows the results obtained from a re-evaluation of the ST method [24, 35], taking excited states with n phonon excitations to be at an energy $n\hbar\omega$ above the ground-state energy in the strong-coupling limit and neglecting quadratic coupling as far as the energy differences are concerned in order to simplify the calculations. For moderate to large values of K, the ST results show that the $K^2 K_{\mathrm{M}}^{(2)}(\Gamma_a \otimes \Gamma_b)$ versus K curves become horizontal straight lines. The asymptotic values can be determined either from the graphs or by taking the strong-coupling limit of the formula for the RFs given in [24] and [35]. However, these asymptotic values are clearly different for $\mathrm{D}_{5\mathrm{d}}$ wells and $\mathrm{D}_{3\mathrm{d}}$ wells, and in both cases the results are different to the FC values. The detailed numerical results from the FC and ST methods in the infinite-coupling limit are collected together in table 1. This table also displays separately the contributions to the RF from the first term in equation (14), denoted by FC_1, and from the second term in (14), denoted by FC_2. We discuss the reasons for these differences in section 5.

4.2. The case of $\Gamma_a \equiv \Gamma_b \equiv H$

On many accounts, this is a much more complicated case than that considered above. The main complication is that the binary multiplication H ⊗ H contains the result 2H, with both components being symmetric. Therefore cases where M = A, T_1, and two H-type components

Table 1. The values of $K^2 K_{\mathrm{M}}^{(2)}(\Gamma_{\mathrm{a}} \otimes \Gamma_{\mathrm{a}})$ for perturbations $\Gamma_a = \mathrm{T_{1g}}$ and $\mathrm{H_g}$, calculated using the FC approach. The contributions from the first and second terms in equation (14) are listed separately as $\mathrm{FC_1}$ and $\mathrm{FC_2}$ respectively, together with their sum FC_{tot}. The values obtained using the ST method in the strong-coupling limit are also given.

Well	M	Γ_{a}	ST	$\mathrm{FC_1}$	$\mathrm{FC_2}$	FC_{tot}
$\mathrm{D_{5d}}$	$\mathrm{A_g}$	$\mathrm{T_{1g}}$	−25/12	−5/6	0	−5/6
	$\mathrm{H_g}$	$\mathrm{T_{1g}}$	−5/6	−1/3	0	−1/3
	$\mathrm{A_g}$	$\mathrm{H_g}$	−5/3	−1/2	0	−1/2
	$\mathrm{H_{1g}}$	$\mathrm{H_g}$	−5/6	−1/3	0	−1/3
	$\mathrm{H_{2g}}$	$\mathrm{H_g}$	−1/6	−1/3	+8/15	+1/5
$\mathrm{D_{3d}}$	$\mathrm{A_g}$	$\mathrm{T_{1g}}$	−5/4	−5/6	0	−5/6
	$\mathrm{H_g}$	$\mathrm{T_{1g}}$	−1/2	−1/3	0	−1/3
	$\mathrm{A_g}$	$\mathrm{H_g}$	−2	−1/2	0	−1/2
	$\mathrm{H_{1g}}$	$\mathrm{H_g}$	−7/6	−1/3	+8/27	−1/27
	$\mathrm{H_{2g}}$	$\mathrm{H_g}$	−1/2	−1/3	0	−1/3

(labelled $\mathrm{H_1}$ and $\mathrm{H_2}$) must all be considered. Also, an orbital operator of H symmetry has non-zero matrix elements within the electronic ground states $|\psi_k(r, Q))$. Thus contributions from the second term in the expression for $G_{FC}^{(k)}$ in equation (14) must be evaluated as well as the contributions from the first term. The detailed results are given in table 1 and figure 3; the table and figure also include the results obtained using the ST method as in the previous section, with a consistent use of the labels $\mathrm{H_1}$ and $\mathrm{H_2}$. The distinguishing labels on H merely reflect the two columns in the tables of [30]. $\mathrm{H_1}$ and $\mathrm{H_2}$ cannot be distinguished on symmetry grounds alone. The problem of repeating irreps has been studied previously in the case of first-order RFs [32, 37, 38] but, to our knowledge, not for second-order RFs. For operators in second-order perturbation theory, the problem should be considered by introducing a phase parameter to describe the mixing of the repeating irreps. However, in general, there are an infinite set of such states. The phase must then be chosen to diagonalize the 2×2 matrix formed by calculating the off-diagonal elements of the second-order perturbation involving both $\mathrm{H_1}$ and $\mathrm{H_2}$ in order to get two real H-type second-order RFs. This very interesting problem has not yet been solved and it will form the subject of future work. The best we can do at the moment is to give the values for $\mathrm{H_1}$ and $\mathrm{H_2}$ separately. In this connection, it is interesting to observe that the difference between $\mathrm{H_1}$ and $\mathrm{H_2}$ arises from the $\mathrm{FC_2}$ contributions in table 1. The contribution from $\mathrm{FC_1}$ involves just the first-order RF $K_{\mathrm{M}}^{(1)}(\mathrm{H})$ divided by the vertical energy gap which is the same for all wells and for all H-type components.

We note that the $\mathrm{FC_2}$ contribution involves the sum $\sum_k c_k^2 (\psi_k | L_{\mathrm{Mm}}^{(2)} | \psi_k)^2$. This sum is the same as that obtained when the intensity of a resonance Raman line for an electric dipole transition is calculated. Moreover, it has the same selection rules as the corresponding quadrupole operator. An additional theoretical point is that $\mathrm{H_1}$ can be associated with an orbital operator $L = 2$ and $\mathrm{H_2}$ from $L = 3$, or vice versa. In the $\mathrm{I_h}$ group there are two kinds of quadrupole moment rather than just one as in the group of general rotations. For $\mathrm{H_1}$, the quadrupole momentum is linked to different axes of symmetry from those linked to $\mathrm{H_2}$. In the trigonal case, the wells are in counter-phase with the quadrupole momentum associated with $\mathrm{H_1}$ but they are in phase with one of the $\mathrm{H_2}$ type. For pentagonal wells, the phase situation is exactly opposite. Therefore, in the trigonal wells all contributions from $(\psi_k | L_{\mathrm{Mm}}^{(2)} | \psi_k)$ cancel for one case and are non-zero for the other case. The situation is exactly opposite for pentagonal wells.

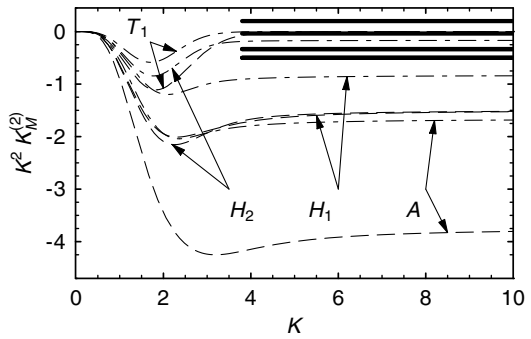

Figure 3. As figure 2, but for perturbations of H symmetry. The solid curves are the results from the FC approximation, given from top to bottom as follows: M = H_2, D_{5d} wells, M = H_1, D_{3d} wells, M = H_1, D_{5d} wells and M = H_2, D_{3d} wells (both degenerate), and M = A, both types of well.

5. FC method in ST basis

It is clear from the figures and tables that the FC results, which are exact in the infinite-coupling limit, are always smaller in magnitude than the values obtained from the ST method. This is because the two methods have different physical bases, as will be explained below. We will also gain further understanding of the reasons contributing to these differences by applying the FC principle to the excited states obtained from the point of view of the ST method.

We will consider first the case of D_{5d} wells. In the ST method, there are six minima at positions $Q = Q_0^k$ (k = 1–6) in the ground sheet. The minima are assumed to be paraboloids (or distorted paraboloids if anisotropic effects are included) centred on $Q = Q_0^k$. The upper sheets are excluded from the calculations, but the arms of the ground parabolic wells are assumed to extend up to infinity. Hence part of all wells $l \neq k$ overlap with each well k. In fact, the potential function for each of the five other wells $l \neq k$ intersect at a point X at $Q = Q_0^k$ which coincides with the centre of the well k. The energy at the intersection point is $12E_{JT}/5$ relative to the bottom of the well. The situation for two D_{5d} wells is represented in figure 4. The figure shows energy as a function of Q in the plane joining two of the D_{5d} minima. The thick dashed curves show the parabolic potential functions to which the two wells are approximated. For clarity, the potential functions for the other four wells are not shown, although they all intersect at the point X. The thick solid lines show the three APESs in this plane.

We can undertake a FC-type calculation in which vertical transitions from one D_{5d} well to the five other D_{5d} wells are considered. Instead of two sheets at an energy of $3E_{JT}$ as in the 'standard' FC approximation, there are now five sheets at energy $12E_{JT}/5$. We have performed this calculation for the $K_{Hg}^{(2)}(T_{1g} \otimes T_{1g})$ RF. It is found that the value for $K^2 K_{Hg}^{(2)}(T_{1g} \otimes T_{1g})$ is exactly the same as the limit of the value obtained from the ST calculation as the coupling tends to infinity. In other words, the FC calculation and the strong-coupling limit of the ST results do give the same answers when the calculation is carried out on the same grounds. This gives us confidence that the FC method in general is a valid approach to use for strong coupling, and that no errors have been made in the calculation.

The values of the RFs obtained using the FC approach described in the last section should be considered to be the most accurate. The result obtained here is obtained on the assumption of a pure parabola in the ground sheet. This assumption is valid near the bottom of the wells, and so is good for the low-lying states. However, figure 4 shows that this is not a good

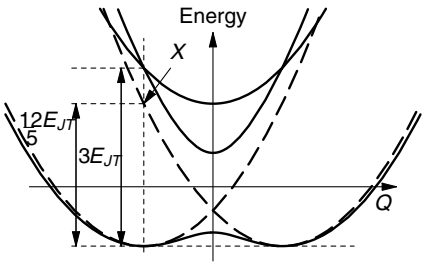

Figure 4. A one-dimensional FC diagram in the plane joining two D_{5d} wells in the lowest sheet of the APES. The thick solid curves show the lowest sheet containing the two wells and the two upper sheets. These upper sheets intersect each other at the minimum values of $Q = Q_0^k$. The vertical energy gap at $Q = Q_0^k$ is $3E_{JT}$. The thick dashed curves show the parabola to which the two wells are approximated in the ST method. The vertical energy gap between the bottom of one well and the upper part of the other well is $12E_{JT}/5$. The parabolas for all of the five D_{5d} wells except the left-hand well intersect at the point X.

approximation for the highly excited states that contribute to the RFs in the strong-coupling limit. As $12E_{JT}/5$ is close to $3E_{JT}$, the main difference between the two FC approaches is that the sum is taken over five sheets for the FC method using the ST basis rather than only two as in the 'standard' FC method. The result is that the ST method of calculation overcounts the contributions to the second-order RFs, as seen in table 1.

The discussion above has focused on D_{5d} wells as these are the easiest to picture. However, a similar situation arises in the case of D_{3d} wells, except that some of the wells to be considered are nearest neighbours and some are next-nearest neighbours. Consequently, there are now three excited sheets at a relative energy of $4E_{JT}/3$ and six sheets at $8E_{JT}/3$. When these numbers are compared to two sheets at $3E_{JT}$ as taken in the 'standard' FC calculation, it can be seen that the ST method will again overestimate the second-order RFs, as seen in table 1.

6. Discussion

We have seen that for the $T_{1u} \otimes h_g$ problem, the ST method has overestimated the second-order RFs in the strong-coupling limit. However, we note that for the cubic T ⊗ e JT system, the values for the second-order RFs obtained by the FC and ST methods coincide with each other and with the results of exact analytical calculations [7]. In retrospect, this can be seen to be somewhat fortuitous. For this problem, there are two excited sheets separated by energy $3E_{JT}$ at the minimum points in both the ST and FC methods. This is a particular feature of the T ⊗ e system. The ST and FC methods are expected to give different answers in other JT systems.

As mentioned above, we have been unable to give a unique definition of the two H-type second-order RFs for the case of the H ⊗ H second-order perturbation. It is possible that this explains why the FC results for D_{3d} wells are different to those obtained for D_{5d} wells for the case of H ⊗ H perturbations. This is in contrast to the results from $T_1 \otimes T_1$ perturbations where the same results are obtained for the two types of well. We would anticipate that the overall structure should depend upon the final symmetry labels only as in the case of $T_1 \otimes T_1$ rather than on details of the symmetry embedded in the underlying calculations. We also note that figure 3 depicts an example in which there are even opposite signs of the H_1 and H_2 components. This is a fascinating problem which is yet to be solved.

In the numerical work of O'Brien [14], a significant coupling between different sheets in the APES was found. Also, her numerical result included significant contributions to RFs from those regions in which two or more excited sheets intersect. Neither these nor the effects of anisotropy have been included in the ST method, as such corrections detract from the idea of a relatively simple analytical calculation. This problem is bypassed in the FC approximation because detailed knowledge of the excited states is not required, and hence these concepts are not relevant.

Finally, the question arises as to which sets of results should be used in any analysis of experimental data. In the intermediate-coupling regime, only results from the ST method are available. There are no alternatives at the present time. The ST method clearly gives results which fit well with the weak-coupling limit of second-order RFs obtained by standard perturbation theory [7]. At the same time, the FC calculations described above show a limitation of the ST results at strong coupling. In this regime, the ST results should be replaced by the FC results. Ultimately, we await reliable experimental data to which our models can be applied.

Acknowledgment

MAG would like to thank the University Research Board of the American University of Beirut for a long-term travel grant.

References

[1] Chancey C C and O'Brien M C M 1997 *The Jahn–Teller Effect in C_{60} and other Icosahedral Complexes* (Princeton, NJ: Princeton University Press)
[2] Bersuker I B and Polinger V Z 1989 *Vibronic Interactions in Molecules and Crystals* (Berlin: Springer)
[3] Stevens K W H 1997 *Magnetic Ions in Crystals* (Princeton, NJ: Princeton University Press)
[4] Bates C A and Stevens K W H 1986 *Rep. Prog. Phys.* **49** 783
[5] Liu X and Miller T A 1992 *Mol. Phys.* **75** 1237
[6] Chibotaru L F 1994 *J. Phys. A: Math. Gen.* **27** 6919
[7] Ham F S 1965 *Phys. Rev.* **138** 1727
[8] Ham F S 1968 *Phys. Rev.* A **166** 307
[9] O'Brien M C M 1969 *Phys. Rev.* A **187** 407
[10] Payne S N and Stedman G E 1983 *J. Phys. C: Solid State Phys.* **16** 2679
[11] Payne S N and Stedman G E 1983 *J. Phys. C: Solid State Phys.* **16** 2705
[12] Payne S N and Stedman G E 1983 *J. Phys. C: Solid State Phys.* **16** 2725
[13] Liu Y M, Kirk P J, Bates C A and Dunn J L 1993 *J. Phys.: Condens. Matter* **5** 5911
[14] O'Brien M C M 1990 *J. Phys.: Condens. Matter* **2** 5539
[15] Ham F S 1972 Jahn–Teller effects in electron paramagnetic resonance spectra *Electron Paramagnetic Resonance* ed S Geschwind (New York: Plenum) pp 1–119
[16] Polinger V Z, Bates C A and Dunn J L 1991 *J. Phys.: Condens. Matter* **3** 513
[17] Bates C A, Dunn J L, Hallam L D, Kirk P J and Polinger V Z 1991 *J. Phys.: Condens. Matter* **3** 3441
[18] Jamila S, Dunn J L and Bates C A 1992 *J. Phys.: Condens. Matter* **4** 4945
[19] Liu Y M, Dunn J L and Bates C A 1994 *J. Phys.: Condens. Matter* **6** 859
[20] Kawamoto T 1997 *Solid State Commun.* **101** 231
[21] Gunnarsson O 1997 *Rev. Mod. Phys.* **69** 575
[22] Bietsch W, Bao J, Ludecke J and van Smaalen S 2000 *Chem. Phys. Lett.* **324** 37
[23] Barckholtz T A and Miller T A *Computational Molecular Spectroscopy* ed P Bunker and P Jensen (New York: Wiley) p 539
[24] Qiu Q C, Dunn J L, Bates C A, Abou-Ghantous M and Polinger V Z 2000 *Phys. Rev.* B **62** 16 155
[25] Herzberg G 1950 *Spectra of Diatomic Molecules* 2nd edn (Princeton, NJ: van Nostrand-Reinhold)
[26] Landau L D and Lifshitz E M 1977 *Quantum Mechanics: Non-Relativistic Theory (Course of Theoretical Physics)* 3rd edn (Oxford: Pergamon)

[27] Abou-Ghantous M, Dunn J L, Polinger V Z and Bates C A 2000 *15th Int. Symp. on the Jahn–Teller Effect (NATO Science Series II, vol 39) (Boston, MA)* ed M Kaplan and G O Zimmerman (Dordrecht: Kluwer)
[28] Grosso G and Pastori-Parravicini 1999 *Solid State Physics* (London: Academic)
[29] Perebeinos V and Allen P B 2000 *Phys. Rev. Lett.* **85** 5178
[30] Fowler P W and Ceulemans A 1985 *Mol. Phys.* **54** 767
[31] Ceulemans A and Fowler P W 1989 *Phys. Rev.* A **39** 481
[32] Cullerne J P and O'Brien M C M J 1994 *J. Phys.: Condens. Matter* **6** 9017
[33] Qiu Q C, Dunn J L, Bates C A and Liu Y M 1998 *Phys. Rev.* B **58** 4406
[34] Dunn J L and Bates C A 1995 *Phys. Rev.* B **52** 5996
[35] Qiu Q Q, Dunn J L, Bates C A and Liu Y M 1999 *14th Int. Symp. on Electron–Phonon Dynamics and Jahn–Teller Effect (Erice, Sicily)* (Singapore: World Scientific) p 273
[36] Longuet-Higgins H C, Öpik U, Pryce M H L and Sack R A 1958 *Proc. R. Soc.* A **244** 1
[37] Cullerne J P, Angelova M N and O'Brien M C M 1995 *J. Phys.: Condens. Matter* **7** 3247
[38] Oliete P B, Bates C A, Dunn J L and Stedman G E 1999 *Phys. Rev.* B **60** 2319